PROCEEDINGS A

rspa.royalsocietypublishing.org

Research

Article submitted to journal

Subject Areas:
Applied mathematics

Keywords:
Porous media, Double-diffusive convection, Mixing, Stability analysis, Heat source

Author for correspondence:
Kirti Chandra Sahu
e-mail: ksahu@iith.ac.in

Linear and nonlinear thermosolutal instabilities in an inclined porous layer

K. Gautam[1], P. A. L. Narayana[1] and Kirti Chandra Sahu[2]

[1] Department of Mathematics, Indian Institute of Technology Hyderabad, Sangareddy 502285, Telangana, India

[2]Department of Chemical Engineering, Indian Institute of Technology Hyderabad, Sangareddy 502 285, Telangana, India

We investigate the double-diffusive instability in an inclined porous layer with a concentration based internal heat source by conducting linear instability and nonlinear energy analyses. The effects of different dimensionless parameters, such as the thermal (Ra_T) and solutal (Ra_S) Rayleigh numbers, the angle of inclination (ϕ), the Lewis number (Le), and the concentration based internal heat source (Q) are examined. A comparison between the linear and nonlinear thresholds for the longitudinal and transverse rolls provides the region of subcritical instability. We found that the system becomes more unstable when the thermal diffusivity is greater than the solute and the internal heat source strength increases. It is observed that the system is stabilised by increasing angle of inclination. While the longitudinal roll remains stationary without the region of subcritical instability, as the angle of inclination increases, the transverse roll switches from stationary-oscillatory-stationary mode. Our numerical results show that for $Ra_S < 0$, for all Q values, the subcritical instability only exists for transverse rolls. For $Ra_S \geq 0$, however, the subcritical instability appears only for $Q = 0$ and $Q \geq 0$, respectively, for longitudinal and transverse rolls.

THE ROYAL SOCIETY PUBLISHING

1. Introduction

The phenomenon of double-diffusive convection (i.e., in the presence of two scalars diffusing at different rates) in saturated porous media is of great practical importance in many disciplines of science and engineering, such as oceanography, chemical engineering, geophysics, geothermal reservoir, food processing, transport of contaminants in saturated soil and underground disposal of nuclear waste, to name a few [1,2]. Thus, several researchers have investigated the instabilities associated with double-diffusive phenomenon in both viscosity [3–6] and density [7] stratified systems. The present study is restricted to the instability in density-stratified flow in an inclined porous media.

A single-component configuration with a denser layer of fluid overlying a less dense layer of fluid is unstable under the action of gravity. However, the configuration is stable if we invert the fluid layers (i.e., if a less dense fluid layer overlays a denser fluid layer). This intuitive argument on the stability of this system is not true in the case of double-diffusive systems. To understand this phenomenon, let us analyse two configurations involving gradients of temperature and solute concentration [8]. (i) A less dense layer of salty and warmer liquid overlying a more dense layer of fresh and cold liquid, and (ii) a less dense layer of cold and fresh liquid overlying a more dense layer of salty and warmer liquid. Based on the discussion above on the single-component system, we expect both the configurations to be stable. However, it is not true in the presence of two species diffusing at different rates. It is well known that temperature diffuses a thousand times faster than salt. In the first configuration, if we displace a small parcel of fluid from less dense top layer (salty and warmer) to the more dense bottom layer (fresh and cold), it will become cold, but will remain salty, thus the density of the displaced parcel will higher than the bottom layer fluid. Therefore, it will continue to penetrate in the downward direction forming a finger. This is commonly known as "fingering" instability in double-diffusive density-stratified systems. In the second configuration, when we displace a small parcel of the top fluid (cold and fresh) into the bottom layer (warmer and salty), it will gain heat faster than salinity, so the displaced parcel will become warm, but will remain fresh. Thus the density of the displaced parcel will become lower than the surrounding bottom fluid. Under the action of buoyancy force, the displaced fluid blob will move in the upward direction and this process will be repeated. This is commonly known as "oscillatory" instability in double-diffusive density-stratified systems.

Following the brief general discussion on the "fingering" and "oscillatory" instabilities in double-diffusive convection, below, we review the previous studies on instability in density-stratified porous media in the context of the present work.

Parthiban and Patil [9] investigated the effect of horizontal temperature gradient on the onset of convection due to non-uniform heating boundaries in the presence of an internal heat source. They observed that the internal heat source leads to the onset of convection. They found that increasing the horizontal temperature gradient destabilises the system. Later, Parthiban and Patil [10] extended their work by considering porous medium to be anisotropic and reported that the longitudinal rolls are the least stable ones with or without the internal heat source. Rionero and Straughan [11] have studied the influence of variable gravity on the onset of convection in the presence of an internal heat source. They found that the principle of stability exchange (which means that the convection happens as stationary convection) holds good in the case of a small variation in gravity and in the presence of an internal heat source. Alex and Patil [12] also have examined the effect of variable gravity on the onset of convection in an anisotropic porous medium with a temperature gradient in the presence of an internal heat source. All these studies are for mono-diffusive (with only one scalar) horizontal systems.

Hill [13] extended the study of the internal heat source from the mono-diffusive to the double-diffusive case in a horizontal porous layer. He performed linear and nonlinear stability analyses in a fluid-saturated porous medium with a concentration based internal heat source. Capone *et al.* [14] investigated the double-diffusive penetrative convection ("fingering" instability) in a fluid-saturated anisotropic horizontal porous layer using internal heat source with throughflow. They

found that increasing the internal heat source destabilises the system. They observed "oscillatory" instability for throughflow between -0.2 to 0.2.

Next, we discuss literature on the instability in inclined mono-diffusive porous layers. Bories and Combarnous [16] theoretically and experimentally studied the thermal convection in an inclined mono-diffusive porous layer. They observed different types of instability patterns of longitudinal rolls and polyhedral cells. Since then this problem has been studied by several researchers (see e.g. [17,18]). Weber [18] found that the principle of stability exchange is valid for small values of channel inclination to the horizontal, ϕ. They found that the threshold Rayleigh number above which the thermal instability occurs to be $4\pi^2/\cos\phi$. Later, in an unstably stratified porous layer, Rees and Bassom [19] reported distinct behaviours of thermal instability at various asymptotic limits. They found the instability to be two-dimensional for small values of ϕ.

Barletta and Storesletten [20] conducted linear instability analysis of an unicellular flow in an inclined enclosure heated from below with constant heat flux and observed that the transverse rolls are most unstable for small inclination angles and small aspect ratios (width-to-height ratio) of the enclosure. Rees and Barletta [21] investigated the instability in an inclined channel with the lower wall subjected to a constant heat flux. The numerical method and the boundary conditions used in these studies are similar to the ones given in Refs. [22] and [23].

Barletta and Rees [24] conducted thermal stability analysis of a Darcy-Hadley flow in an inclined porous channel. They found that an increase in the inclination angle of the channel destabilises and stabilises the flow when the top wall is colder and hotter than the bottom wall, respectively. Nield *et al.* [25] analysed the effect of viscous dissipation on the onset of convection in an inclined porous channel and observed that the viscous dissipation plays a vital role in case of convectively unstable system. An extensive review of the literature dealing with flows in inclined porous layers and convection in porous media can be found in Refs. [26–28]. The effect of internal heat source based on concentration on the instability of the flow in an inclined porous layer was studied by Barletta *et al.* [29] considering the top wall at an isothermal condition and bottom wall to be adiabatic or maintaining both the walls at different temperatures (isothermal). Also, few studies used the energy-based nonlinear method to investigate the stability of flow in an inclined mono-diffusive porous layer (see, e.g. [34–36]) although in the context of carbon sequestration and thermal convection.

Although several authors have investigated the instability in inclined mono-diffusive porous layer using linear and nonlinear theories, as discussed above, only recently, Matta and Hill [30] performed a linear instability analysis of double-diffusive convection in an inclined porous layer where concentration and temperature have destabilising and stabilising influences, respectively. Thus, in the configuration considered by Matta and Hill [30], it is difficult to predict whether the instability observed is solely due to the double-diffusive convection or due to the combined effect of the double-diffusive convection and the imposed unstable stratification of the solute.

The above-mentioned review reveals that the double-diffusive phenomena in inclined porous layers have been mostly investigated via linear instability analysis, which provides a sufficient condition for the occurrence of instability. On the other hand, by conducting an energy-based nonlinear theory, one can get the sufficient condition for stability. Thereby identifying the region between the thresholds obtained from the nonlinear and linear instability analyses, which is known as the region of subcritical instability. Thus considering the importance of the nonlinear analysis, in this study we attempt to understand the double-diffusive convection in an inclined channel due to the presence of concentration of a solute and temperature by conducting both linear and nonlinear analyses. Both the analyses yield generalised eigenvalue problems, which are then solved numerically by using the Chebyshev-tau method coupled with QZ-algorithm [37,38]. We have also compared the threshold Rayleigh numbers obtained from the linear and nonlinear analyses.

The main motivation for this work is to identify the existence of the region of subcritical instability, if any, in an inclined porous layer. The flow problem is governed by a large parameter space consisting of thermal and solutal Rayleigh numbers (Ra_T & Ra_S), the angle of inclination

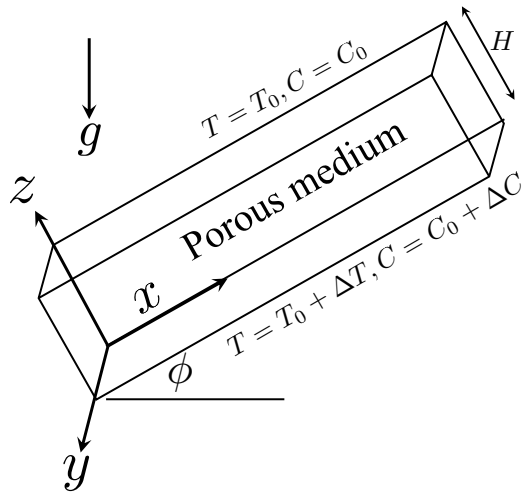

Figure 1. Schematic diagram of the flow in an inclined porous layer. The top and bottom walls are rigid and separated by a distance of H. ϕ is the angle of inclination of the porous layer to the horizontal. Note that the channel is infinitely long in the x direction.

(ϕ), the diffusivity ratio characterised by the Lewis number (Le) and the internal heat source parameter (Q) due to the solute in the medium. We found that the flow stability undergoes some qualitative changes due to the combined effect of these parameters. An interesting finding of the present study is that the longitudinal rolls remain stationary while the transverse rolls transform from a stationary to an oscillatory mode and revert to a stationary mode with an increase in the angle of inclination of the porous layer. Although the transverse roll instability is preferred, these rolls lead to the region of subcritical instability.

The rest of the article is organised as follows. The problem is formulated in Section 2, wherein the basic state, the linear and nonlinear stability equations are provided and the associated dimensionless numbers are presented. The linear and nonlinear stability results are discussed in Section 3 and concluding remarks are given in Section 4.

2. Formulation

We investigate the linear and nonlinear stability characteristics of flow through an inclined porous medium, with an angle of inclination to the horizontal ϕ, of height H in the presence of temperature (T) and concentration (C) gradients. The temperature and concentration at the top and bottom layers are fixed at T_0, C_0, and $T_0 + \Delta T, C_0 + \Delta C$, respectively. Note that a positive value of ΔC and a negative value of ΔT imply a stable configuration, and vice versa. A Cartesian coordinate system (x, y, z) is used, wherein x, y and z denote the streamwise, the spanwise and the wall-normal coordinates, respectively. The schematic diagram of the flow configuration is shown in Fig. 1. Gravity acts in the negative vertical direction. The working fluid is assumed to be Newtonian and incompressible. The viscosity, μ of the fluid is assumed to be constant and the density of the fluid, ρ depends on the temperature and concentration as follows:

$$\rho(T, C) = \rho_0 \left(1 - \beta_T (T - T_0) + \beta_C (C - C_0)\right), \tag{2.1}$$

where ρ_0 is the reference density at $T = T_0$ and $C = C_0$; β_T and β_C are the thermal and solutal expansion coefficients, respectively.

The flow dynamics is governed by the continuity, Darcy's, energy and convective diffusion equations, which are given by

$$\nabla \cdot \mathbf{u} = 0, \tag{2.2}$$

$$\tfrac{\mu}{K}\mathbf{u} = -\nabla P - \rho g\left(\sin(\phi)\hat{i} + \cos(\phi)\hat{k}\right), \tag{2.3}$$

$$M\left(\tfrac{\partial T}{\partial t}\right) + \mathbf{u}\cdot\nabla T = \alpha_T \nabla^2 T + Q_d(C - C_0), \tag{2.4}$$

$$\psi\left(\tfrac{\partial C}{\partial t}\right) + \mathbf{u}\cdot\nabla C = \alpha_C \nabla^2 C, \tag{2.5}$$

where $\mathbf{u}(u, v, w)$ is the Darcy velocity field, wherein u, v and w are the components of the velocity in x, y and z directions, respectively; P is the pressure field; K is the permeability of the porous media; α_T and α_C are effective thermal and solutal diffusion coefficients, respectively; M and ψ are the ratios of the specific heat capacity of saturated porous medium to the specific heat capacity of saturating fluid and porosity, respectively; $\hat{i}$ and $\hat{k}$ are the unit vectors in x and z directions, respectively; $Q_d(\equiv Q_{int}/(\rho_0 c_p)_f)$, where Q_{int} is the volumetric rate of heat production within the porous medium (W/m^3) and c_p is the specific heat at constant pressure of the fluid (J/(kg ·K).

The above equations are non-dimensionalised as follow

$$(\widetilde{x}, \widetilde{y}, \widetilde{z}) = (x/H, y/H, z/H),\ \widetilde{t} = \left(\alpha_T/MH^2\right)t,\ \widetilde{\mathbf{u}} = \mathbf{u}\,(H/\alpha_T),$$
$$\widetilde{T} = T/\Delta T,\ \widetilde{C} = C/\Delta C,\ \widetilde{T_0} = T_0/\Delta T,\ \widetilde{C_0} = C_0/\Delta C,\ \widetilde{P} = P\,(K/\mu\alpha_T), \tag{2.6}$$

resulting in the following dimensionless equations (hereafter dropping tilde notations).

$$\nabla \cdot \mathbf{u} = 0, \tag{2.7}$$

$$\mathbf{u} = -\nabla P - (\mathcal{G} - Ra_T(T - T_0) + Ra_C(C - C_0))\left(\sin(\phi)\hat{i} + \cos(\phi)\hat{k}\right), \tag{2.8}$$

$$\tfrac{\partial T}{\partial t} + \mathbf{u}\cdot\nabla T = \nabla^2 T + Q(C - C_0), \tag{2.9}$$

$$\psi' \tfrac{\partial C}{\partial t} + \mathbf{u}\cdot\nabla C = \tfrac{1}{Le}\nabla^2 C, \tag{2.10}$$

where $Q\left(\equiv Q_d \Delta C H^2/\alpha_T \Delta T\right)$ is the dimensionless concentration based internal heat source, $\mathcal{G}\,(\equiv \rho_0 g K H/\mu\alpha_T)$ is the dimensionless gravity term, $Ra_T(\equiv \rho_0 g \beta_T K H \Delta T/\mu\alpha_T)$ is the thermal Rayleigh number and $Ra_S\,(\equiv \rho_0 g \beta_C K H \Delta C/\mu\alpha_C)$ is the solutal Rayleigh number, and $Le\,(\equiv \alpha_T/\alpha_C)$ is the Lewis number. Following the previous studies, the value of $\psi' \equiv \psi/M$ is taken to be 1 in the present study [39].

The governing dimensionless equations (Eqs. (2.7) - (2.10)) are subjected to the following boundary conditions:

$$w = 0,\ T = 1 + T_0,\ C = 1 + C_0 \text{ at } z = 0, \tag{2.11}$$

$$w = 0,\ T = T_0,\ C = C_0 \text{ at } z = 1. \tag{2.12}$$

(a) Basic state

The basic state corresponds to a steady, parallel, fully-developed flow $(u_b(z), 0, 0)$. As there is no net flow in the x direction, we have $\int_0^1 u_b dz = 0$, and the dimensionless equations for $u_b(z)$, $T_b(z)$ and c_b are given by

$$u_b(z) = \left[\tfrac{Ra_T Q}{24}(4z^3 - 12z^2 + 8z - 1) + \left(Ra_T - \tfrac{Ra_S}{Le}\right)(0.5 - z)\right]\sin(\phi), \tag{2.13}$$

$$T_b(z) = \tfrac{Q}{6}(z^3 - 3z^2 + 2z) + 1 - z + T_0 \tag{2.14}$$

$$C_b(z) = -z + 1 + C_0. \tag{2.15}$$

(b) Linear instability analysis

We conduct the linear instability analysis of the basic flow given by Eqs (2.13)-(2.15) to infinitesimal perturbations by expressing each flow variable as a sum of the basic state and a time-dependent perturbation (designated by a hat):

$$\mathbf{u} = \mathbf{u}_b + \hat{\mathbf{u}}_p,\ P = P_b + \hat{p},\ T = T_b + \hat{\theta},\ C = C_b + \hat{\Phi}, \tag{2.16}$$

where $\hat{\mathbf{u}}_p = (\hat{u}_p, \hat{v}_p, \hat{w}_p)$, $\hat{\theta}$ and $\hat{\Phi}$ are the perturbation velocity, temperature and concentration fields, respectively. We then imposed the following normal mode approach by splitting the disturbance into an amplitude and time-dependent components as

$$[\hat{\mathbf{u}}_p, \hat{\theta}, \hat{\Phi}, \hat{p}] = [\mathbf{u}_p(z), \theta(z), \Phi(z), p(z)] e^{i(a_x x + a_y y)} e^{\sigma t}, \tag{2.17}$$

where $i \equiv \sqrt{-1}$, a_x, a_y and σ are the wavenumbers in the streamwise and the spanwise directions (real), and the frequency (complex) of the perturbation, respectively. Here, $a(\equiv \sqrt{{a_x}^2 + {a_y}^2})$ is the overall wave number and σ denotes growth rate parameter ($\sigma \in \mathbb{C}$). We can write $\sigma = \sigma_r + i\sigma_i$ where the subscripts r and i represent the real and the imaginary parts, such that if σ_r is positive then the perturbation grows exponentially with time, but the negative value represents the perturbation decays exponentially to 0 as $t \to \infty$. We assume that the perturbations $(\hat{\mathbf{u}}_p, \hat{\theta}, \hat{\Phi}, \hat{p})$ defined on $\mathbb{R}^2 \times [0,1]$ are periodic with periods $2\pi/a_x$ and $2\pi/a_y$ in x and y directions, respectively. The periodicity cell is denoted by $\Omega = [0, 2\pi/a_x] \times [0, 2\pi/a_y] \times [0,1]$. The longitudinal and transverse rolls are represented by $a_x = 0$ and $a_y = 0$, respectively.

Following the standard procedure [40]: (i) substitution of Eq. (2.17) into Eqs. (2.7)-(2.10), (ii) subtraction of the basic state solutions, and (iii) linearization and elimination of the pressure perturbation, we obtained the following linear instability equations (suppressing the hat notations):

$$(D^2 - a^2)w + \left(a^2 \cos(\phi) + i a_x D \sin(\phi)\right)\left(Ra_T \theta - \frac{Ra_S}{Le}\Phi\right) = 0, \tag{2.18}$$

$$\left(D^2 - a^2 - i a_x G(z)\right)\theta - F(z) w + Q\Phi = \sigma\theta, \tag{2.19}$$

$$\left[\frac{1}{Le}(D^2 - a^2) - i a_x G(z)\right]\Phi + w = \sigma\Phi, \tag{2.20}$$

where $D = d/dz$, and

$$F(z) = \frac{Q}{6}(3z^2 - 6z + 2) - 1, \tag{2.21}$$

$$G(z) = \left[\frac{Ra_T Q}{24}\left(4z^3 - 12z^2 + 8z - 1\right) + \left(Ra_T - \frac{Ra_S}{Le}\right) \times (0.5 - z)\right] \sin(\phi). \tag{2.22}$$

Eqs. (2.18) - (2.20) are subjected to the following boundary conditions

$$w = 0,\ \theta = 0,\ \Phi = 0 \ \text{ at } z = 0, 1. \tag{2.23}$$

The system of Eqs. (2.18) $-$ (2.23) constitutes a sixth-order differential eigenvalue problem for the vertical thermal Rayleigh number Ra_T. It is solved by using the Chebyshev-tau method which is coupled with $QZ-$ algorithm [37,38]. The threshold value of thermal Rayleigh number for linear theory is defined for longitudinal rolls (i.e. $a_x = 0$) and transverse rolls (i.e. $a_y = 0$)

$$Ra_{T_L} = \min_{a_x, a_y} Ra_T(a_x, a_y, Ra_S, Q, Le, \phi). \tag{2.24}$$

The linear instability theory offers a necessary criterion for instability, i.e. it provides the Rayleigh number above which the flow is unstable (upper limit). On the other hand, using the energy-based nonlinear stability theory, we get the sufficient condition for the stability of the system, i.e. when subjected to small disturbances, one can get the Rayleigh number below which the flow is stable (lower limit). In what follows, we present the nonlinear stability analysis.

The linear instability and nonlinear stability analyses typically yield different thresholds at the onset. However, if the eigenvalue problem in the case of the linear instability theory is self-adjoint (so that we can set $\sigma = 0$), then both the linear and nonlinear energy theories provide the

same threshold value. The reason for this is that the Euler-Lagrange equations in the nonlinear theory are identical to the linear instability equations [32,33]. In the case of the double-diffusive convection, we get a system that is not self-adjoint.

(c) Nonlinear stability analysis

The nonlinear energy stability analysis is conducted in a space $L^2(\Omega)$, where $L^2(\Omega)$ consists of all measurable functions g in Ω, such that $\int_\Omega |g|^2 dv$ is finite. The following procedure is followed in order to derive the governing nonlinear stability analysis. First elimination of the pressure term from the perturbed momentum (Darcy's) equations (i.e. the resultant equations obtained by substituting Eqs. (2.16) and (2.17) in Eq. (2.8) and subtracting of the corresponding basic state solutions), yields

$$\nabla^2 w + \left(D\frac{\partial}{\partial x}\sin(\phi) - \nabla_1^2 \cos(\phi) \right) \left(Ra_T \theta - \frac{Ra_S}{Le}\Phi \right) = 0. \tag{2.25}$$

where $\nabla_1^2 = \partial^2/\partial x^2 + \partial^2/\partial y^2$.

Then following the same procedure for Eqs. (2.9) and (2.10) and then multiplying the resultant perturbed energy and convective-diffusion equations by the conjugate of $\hat{\theta}$ and $\hat{\Phi}$, and integrating over the periodic cell Ω, we obtain

$$\tfrac{1}{2}\tfrac{d}{dt}\|\hat{\theta}\|^2 = -\|\nabla\hat{\theta}\|^2 + Q\langle\hat{\Phi},\hat{\theta}\rangle - \langle F(z)\hat{w},\hat{\theta}\rangle - \tfrac{1}{2}\int_\Omega G(z)\tfrac{\partial\hat{\theta}^2}{\partial x}d\Omega, \tag{2.26}$$

$$\tfrac{1}{2}\tfrac{d}{dt}\|\hat{\Phi}\|^2 = -\tfrac{1}{Le}\|\nabla\hat{\Phi}\|^2 + \langle\hat{w},\hat{\Phi}\rangle - \tfrac{1}{2}\int_\Omega G(z)\tfrac{\partial\hat{\Phi}^2}{\partial x}d\Omega, \tag{2.27}$$

where $\|\cdot\|$ and $\langle\cdot,\cdot\rangle$ denotes the norm and the inner product defined on $L^2(\Omega)$, respectively. Now we define an energy functional $E(t)$ as

$$E(t) = \frac{1}{2}\|\hat{\theta}\|^2 + \xi\frac{1}{2}\|\hat{\Phi}\|^2, \tag{2.28}$$

where ξ is a positive coupling parameter that has to be selected optimally. Differentiating the energy functional, $E(t)$ with respect to t, and utilising Eqs. (2.26) and (2.27), yields the following identity

$$\frac{dE}{dt} = \mathcal{I} - \mathcal{D}, \tag{2.29}$$

where

$$\mathcal{I} = Q\langle\hat{\Phi},\hat{\theta}\rangle - \langle F(z)\hat{w},\hat{\theta}\rangle + \xi\langle\hat{w},\hat{\Phi}\rangle - \frac{1}{2}\int_\Omega G(z)\frac{\partial}{\partial x}(\hat{\theta}^2 + \xi\hat{\Phi}^2)d\Omega, \tag{2.30}$$

$$\mathcal{D} = \|\nabla\hat{\theta}\|^2 + \frac{\xi}{Le}\|\nabla\hat{\Phi}\|^2. \tag{2.31}$$

We now define a maximisation problem as

$$\frac{1}{R_E} = \max_{\mathcal{H}}\frac{\mathcal{I}}{\mathcal{D}}, \tag{2.32}$$

where $\mathcal{H}$ is the space of all admissible perturbations to the corresponding resultant perturbed system of Eqs. (2.8) − (2.10), such that

$$\mathcal{H} = \left\{ (\hat{\mathbf{u}},\hat{\theta},\hat{\Phi}) \in L^2(\Omega) : \nabla\cdot\hat{\mathbf{u}} = 0, \hat{w} = \hat{\theta} = \hat{\phi} = 0 \text{ at } z = 0,1 \right\}, \tag{2.33}$$

then Eq. (2.29) can be written as

$$\frac{dE}{dt} \le -\mathcal{D}\left(1 - \frac{1}{R_E}\right). \tag{2.34}$$

Upon utilising the Poincare inequality (for any $N \in W_0^{1,2}(\Omega)$, such that $\pi^2\|N\|^2 \le \|\nabla N\|^2$ where Ω is smooth bounded domain) on $\mathcal{D}$, we deduce that $\mathcal{D} \ge rE$ for some constant $r > 0$. After

integrating Eq. (2.34), we obtain

$$E(t) \leq E(0)e^{-\chi rt}, \tag{2.35}$$

where $\chi = \frac{R_E - 1}{R_E}$, for all $R_E > 1$ and $E(t) \to 0$ as $t \to \infty$. Clearly, it shows that the decay of $\hat{\Phi}$ and $\hat{\theta}$ follow by the definition of $E(t)$.

For the global nonlinear stability analysis, the decay of $\hat{\mathbf{u}}_p$ must also be demonstrated. In order to achieve this, we first multiply the resultant perturbed momentum (Darcy's) equations by the conjugate of $\hat{\mathbf{u}}_p$ on both sides and integrating over the periodicity cell Ω to get

$$\|\hat{\mathbf{u}}_p\|^2 = Ra_T \sin\phi \langle \hat{\theta}, \hat{u}_p \rangle + Ra_T \cos\phi \langle \hat{\theta}, \hat{w}_p \rangle - \frac{Ra_S}{Le} \sin\phi \langle \hat{\Phi}, \hat{u}_p \rangle - \frac{Ra_S}{Le} \cos\phi \langle \hat{\Phi}, \hat{w}_p \rangle. \tag{2.36}$$

By using *AM–GM* inequalities in the above, we derive

$$\|\hat{\mathbf{u}}_p\|^2 \leq \frac{1}{2}(\epsilon + \epsilon_1 + \epsilon_2 + \epsilon_3)\|\hat{\mathbf{u}}_p\|^2 + \frac{Ra_T^2}{2}\left(\frac{\sin^2\phi}{\epsilon} + \frac{\cos^2\phi}{\epsilon_2}\right)\|\hat{\theta}\|^2 + \frac{Ra_S^2}{2Le^2}\left(\frac{\sin^2\phi}{\epsilon_1} + \frac{\cos^2\phi}{\epsilon_3}\right)\|\hat{\Phi}\|^2, \tag{2.37}$$

where $\epsilon, \epsilon_1, \epsilon_2$ and ϵ_3 are positive constants. In particular, choosing the values for the constants $\epsilon = \epsilon_1 = \epsilon_2 = \epsilon_3 = 1/3$, we obtain

$$\|\hat{\mathbf{u}}_p\|^2 \leq \frac{9}{2} Ra_T^2 \|\hat{\theta}\|^2 + \frac{9}{2}\frac{Ra_S^2}{Le^2}\|\hat{\Phi}\|^2. \tag{2.38}$$

The decay of $\hat{\mathbf{u}}_p$ clearly follows by the definition of $E(t)$ as $\hat{\theta} \to 0$ and $\hat{\Phi} \to 0$ in the stability measure $L^2(\Omega)$ as $t \to \infty$.

We now introduce the Euler-Lagrange parameter, Λ in Eq. (2.25), such that

$$\Lambda(\mathbf{x})\left(\nabla^2 w + \left(D\frac{\partial}{\partial x}\sin(\phi) - \nabla_1^2 \cos(\phi)\right)\left(Ra_T\theta - \frac{Ra_S}{Le}\Phi\right)\right) = 0. \tag{2.39}$$

Assuming the threshold condition, $R_E = 1$, in the maximization problem and adopting the normal mode (Eq. (2.17)) as in linear instability analysis, the system of the Euler-Lagrange equations for the maximization problem are given by

$$(D^2 - a^2)w + \left(a^2\cos(\phi) + ia_x D\sin(\phi)\right)\left(Ra_T\theta - \tfrac{Ra_S}{Le}\Phi\right) = 0, \tag{2.40}$$

$$(D^2 - a^2)\Lambda - F(z)\theta + \xi\Phi = 0, \tag{2.41}$$

$$\left(2(D^2 - a^2) - ia_x G(z)\right)\theta - F(z)w + Q\Phi + Ra_T\left(a^2\cos(\phi) + ia_x D\sin(\phi)\right)\Lambda = 0, \tag{2.42}$$

$$\left(\tfrac{2}{Le}(D^2 - a^2) - ia_x G(z)\right)\Phi + w + \tfrac{Q}{\xi}\theta - \tfrac{Ra_S}{\xi Le}\left(a^2\cos(\phi) + ia_x D\sin(\phi)\right)\Lambda = 0. \tag{2.43}$$

The governing equations for the nonlinear system (Eqs. (2.40)-(2.43)) are subjected to the following boundary conditions:

$$w = 0, \quad \Lambda = 0, \quad \theta = 0, \quad \Phi = 0 \ \text{ at } \ z = 0, \tag{2.44}$$

$$w = 0, \quad \Lambda = 0, \quad \theta = 0, \quad \Phi = 0 \ \text{ at } \ z = 1. \tag{2.45}$$

Eqs. (2.40)-(2.45) constitute an eighth-order differential eigenvalue problem for the thermal Rayleigh number, Ra_T and it is numerically solved by using the Chebyshev-tau spectral method coupled with $QZ-$algorithm [37,38]. The threshold thermal Rayleigh number for nonlinear theory is defined for longitudinal rolls (i.e. $a_x = 0$) and transverse rolls (i.e. $a_y = 0$)

$$Ra_{T_E} = \max_{\xi} \min_{a_x, a_y} Ra_T(\xi, a_x, a_y, Ra_S, Q, Le, \phi). \tag{2.46}$$

It is to be noted here that the numerical results are found to be correct up to 6 decimal places with the inclusion of 40 terms in the Chebyshev-tau polynomial. It can be seen in Table 1 that for the number of terms $n \geq 40$, the scheme used in the present study provides grid-independent results for both the longitudinal and transverse rolls. However, the computational time increases significantly as we increase the value of n. Thus we use $n = 40$ to generate the rest of the results presented in the present study. In addition, when we set $Q = 0$, $Le = 1$, $\phi = 0$ and $Ra_S = 0$, the

Table 1. Effect of number of terms, n in the Chebyshev-tau polynomial on the threshold values of Ra_T evaluated for the longitudinal and transverse rolls for $Le = 1$, $Ra_S = -10$, $Q = 2$ and $\phi = 30^\circ$.

n	Ra_T (longitudinal)	Ra_T (transverse)
40	30.7392	47.5428
50	30.7392	47.5428
50	30.7392	47.5428

configuration reduces to a pure thermal problem, and we found that the threshold value of thermal Rayleigh number, $Ra_{T_c} = 39.47841$, which is the same as $4\pi^2$ [18]. A similar method was previously used in Refs. [15,41].

3. Results and discussion

We begin the presentation of our linear and nonlinear stability results by investigating the effect of the solutal Rayleigh number, Ra_S on the threshold thermal Rayleigh number, Ra_T in Fig. 2 in an inclined porous medium with $\phi = 30^\circ$. The linear and nonlinear stability characteristics in the absence of $(Q = 0)$ and the presence of a concentration based internal heat source with $Q = 2$ are investigated in Figs. 2(a,b) and (c,d), respectively. Note that increasing the concentration increases the density of the fluid, whereas increasing the temperature decreases the density of the fluid (see Eq. (2.1)). Thus, a positive (negative) value of Ra_S $(\equiv \rho_0 g \beta_C K H \Delta C / \mu \alpha_C)$ represents a situation where the concentration of the solute decreases (increases) along the wall-normal direction, and thereby has a stabilising (destabilising) influence. Similarly, positive values of Ra_T $(\equiv \rho_0 g \beta_T K H \Delta T / \mu \alpha_T)$ (as considered in this study) represents the destabilising effect due to temperature. This is true only in the context of the single-component system as discussed in the introduction. We investigate the instability behaviour in the presence of both solute and temperature simultaneously. This double-diffusive phenomenon is characterised by the Lewis number, Le $(\equiv \alpha_T / \alpha_C)$, which is the ratio between the thermal and solutal diffusion coefficients.

In this study we use a fixed notation to represent the results of linear and nonlinear stability, so that the solid line with open symbols represents the results of linear instability, while the dashed line with filled symbols represents the results of nonlinear stability.

Figs. 2(a,b) and (c,b) present the variations of the threshold Ra_T versus Le for different values of Ra_S for $Q = 0$ and $Q = 2$, respectively, such that panels (a), (c) are for the longitudinal $(a_x = 0)$, and (b), (d) are for the transverse $(a_y = 0)$ rolls. Two values of $Ra_S = -10$ and 10 are considered, which represent destabilising and stabilising behaviours due to solute in the system, respectively. Thus, as expected, it can be seen in Figs. 2(a,b) and (c,b) that the threshold Ra_T for the linear and nonlinear instabilities for $Ra_S = -10$ is less than the corresponding threshold Ra_T for $Ra_s = 10$ for both the longitudinal and the transverse rolls for the range of Le considered.

We discuss the results from the linear instability analysis first for $Q = 0$ (without the concentration based internal heat source). It can be seen in Fig. 2(a) that for $Q = 0$, the value of Ra_T for the longitudinal roll is constant $(Ra_T = 35.585)$ for the entire range of Le for $Ra_S = -10$, which is lower than that for $Ra_S = 10$. $Ra_S = 0$ represents the mono-diffusive system, and threshold $Ra_T = 45.585$ (not shown) which is higher than that $Ra_S = -10$. For $Ra_S = 10$, the threshold Ra_T $(Ra_T = 55.585)$ is not a function of Le for $Le \leq 5$, but decreases with further increase in Le. Increasing the value of Le signifies an increase in the value of thermal diffusivity. Thus for a high value of Le, the temperature of the system at the interior tends to become uniform, thus increasing the gradient of temperature near the walls. This, in turn, destabilises the system, i.e., the system becomes unstable to the longitudinal roll at a lower value of Ra_T. On the other hand, for $Q = 0$ (see Fig. 2(b)), the threshold Ra_T for the transverse roll is higher than that of the corresponding value of the longitudinal roll at a fixed Le for both the values of Ra_S taken. This indicates that the transverse rolls (Fig. 2(b)) for the same set of parameters are more stable than the longitudinal rolls (Fig. 2(a)). It can be seen in Fig. 2(b) that for $Ra_S = -10$, increasing

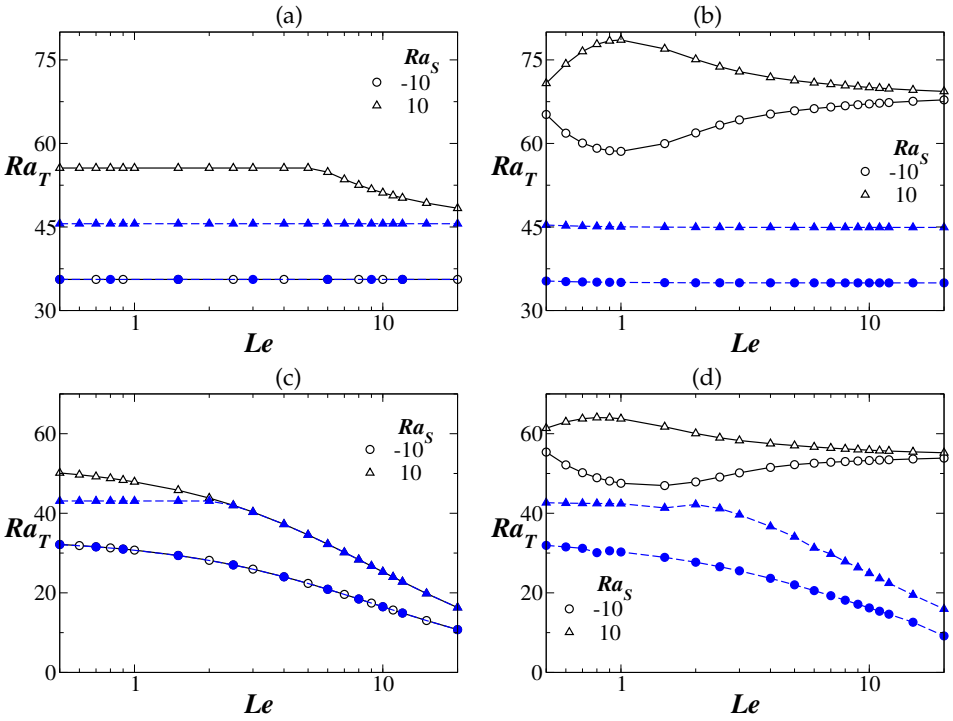

Figure 2. Variations of the threshold thermal Rayleigh number (Ra_T) versus the Lewis number (Le) for different values of the solutal Rayleigh number (Ra_S) obtained using the linear instability analysis (open black symbols) and the nonlinear stability analysis (filled blue symbols). The angle of inclination of the porous layer is $\phi = 30°$. (a,b) $Q = 0$ and (c,d) $Q = 2$, such that (a,c) are for the longitudinal rolls and (b,d) are for the transverse rolls.

Le up to 1 decreases the value of Ra_T because of unstable stratification of the solute (upper plate is more concentrated than the lower plate) and solutal diffusion is higher than the thermal diffusion (so transport of solute from the region of high concentration to lower concentration happens quickly, hence destabilisation occurs). But increasing Le (> 1) further (i.e when thermal diffusion is higher than the solute diffusion) increases the threshold value of Ra_T which stabilised the system. However, for $Ra_S = 10$ increasing the value of Le up to 1, increases the value of Ra_T which has a stabilisation effect on the system due to high concentration at the lower boundary and less thermal diffusion. But when the value of Le increases further (i.e. > 1), the threshold value of Ra_T decreases as a result of higher thermal diffusion which destabilises the system. After a certain value of Le, for $Ra_S = -10$ and $Ra_S = 10$, the threshold value of Ra_T eventually reaches to the same asymptotic value for the situation considered in the present study.

The stability curves for longitudinal rolls obtained from the nonlinear stability analysis follow similar trends as those of linear instability analysis, which is evident from Figs. 2(a) and (c). In the absence of the concentration based internal heat source, $Q = 0$ (see Fig. 2(a)), it can be seen that for the negative value of Ra_S, the results from both the linear and nonlinear theories coincide and there is no region of subcritical instability. This shows that linear instability analysis is sufficient to understand the onset of convection in the absence of concentration based internal heat source. However, the situation is different for the positive value of Ra_S for the set of parameters considered. In this case, the region of subcritical instability exists and more widened up to $Le \leq 5$, and thereafter it starts to decrease for larger values of Le. Hence for higher values of Le, there will be less chance of having the region of subcritical instability in the system.

The variation of Ra_T versus Le in the presence of concentration based heat source $(Q = 2)$ for the longitudinal and transverse rolls are shown in Figs. 2(c) and (d), respectively. A finite value

of Q inherently implies a finite value of Ra_S. In this case, increasing Le decreases the threshold value of Ra_T at the onset of the instability for both positive and negative values of Ra_S (i.e. $Ra_S = -10$ and $Ra_S = 10$) for the longitudinal rolls. In the presence of the concentration based internal heat source ($Q = 2$), the threshold value of Ra_T is less than that in the absence of Q. Therefore, in the presence of Q, longitudinal rolls are more unstable than in the absence of Q. It can be observed that increasing the value of Ra_S stabilises the flow. Comparison of Figs. 2(a) and (c) reveals that concentration based internal heat source destabilises the system via increasing the gradient of concentration near the walls. In Fig. 2(d), we observe that the stability curves follow the same trend as in Fig. 2(b), and the threshold value of Ra_T is less than the threshold value in Fig. 2(b). However for the transverse rolls in the absence of Q (Fig. 2(b)), it is observed that for the negative value of Ra_S the region of subcritical instability exist and is decreased up to $Le = 1$ and thereafter it starts to increase. But for positive value of Ra_S, the region of the subcritical instability increases for the lower values of $Le(< 1)$ and subsequently decreases. From this, it is clear that both positive and negative values of Ra_S can push the system to a subcritical state even in the absence of concentration based internal heat source, Q. In the presence of concentration based internal heat source $(Q = 2)$ (see Fig. 2 (c)), it is observed that for negative value of Ra_S, the region of subcritical instability is negligible for longitudinal rolls and we can conclude that linear instability analysis is sufficient to predict the onset of convection for the longitudinal rolls.

On the other hand, the nonlinear stability threshold decreases as the values of Ra_S and Le are increased for the transverse rolls in the presence of Q. This observation is in contrast to the results obtained in the linear theory. It is also noted that the region of the subcritical instability increases as the value of Ra_S decreases as shown in Fig. 2d.

Next, we discuss the effect of the inclination of the porous medium on the linear and nonlinear stability characteristics of the flow. Figs. 3(a,b) and (c,d) present the variation of the threshold Ra_T versus the angle of inclination to the horizontal, ϕ for different values of the solutal Rayleigh number, Ra_S for $Q = 0$ and $Q = 2$, respectively. The panels (a,c) and (b,d) are for longitudinal and transverse rolls, respectively. Here, $Le = 10$ and thus the thermal diffusion is more than the solutal diffusion. As discussed in the introduction section, in a horizontal porous channel ($\phi = 0$), Hill [13] observed destabilization for negative values of the solutal Rayleigh number, Ra_S. It can be seen in Fig. 3(a) that for $Ra_S = -10$, increasing the value of ϕ increases the threshold thermal Rayleigh number, Ra_T associated with the longitudinal rolls obtained from both the linear and nonlinear theories. In this case, $g\sin\phi$ and $g\cos\phi$ act along the negative x and negative z directions, respectively. This reduces the effective unstable density stratification in the wall-normal direction; thus stabilising. This phenomenon is also observed when the concentration at the lower boundary is more than that at the upper boundary (i.e., $Ra_S = 10$). It can, therefore, be concluded that the onset of convection can be delayed as the angle of inclination of the porous channel increases.

In the case of the transverse rolls (Fig. 3(b)), although the instability curve for $Ra_S = -10$ follows the same trend as that of Fig. 3(a), the threshold value of Ra_T increases faster than the longitudinal rolls as ϕ is increased. For $Ra_S = 10$ and for higher thermal diffusion ($Le = 10$), the threshold value of Ra_T increases as the inclination angle of ϕ increases. It is also interesting to note that, for the case of the transverse roll with $Q = 0$, the stationary transverse rolls exist between $\phi = 0^\circ$ and $\phi \approx 4^\circ$, but at around $\phi \approx 4^\circ$ (marked as kink 1 in Fig. 3(b)) convection switches from the stationary transverse rolls to the travelling transverse rolls for up to $\phi \approx 5.7^\circ$ (marked as kink 2 in Fig. 3(b)). Then after that again the convective instability is in the form of the stationary transverse rolls. Thus, in contrast to the mono-diffusive inclined porous layer, where the only preferred mode is the stationary one [19], in the double-diffusive case, both the stationary and the oscillatory modes exist. Close inspection of Figs. 3(a) and (b) reveals that the rates of increase of Ra_T with ϕ for $Ra_S = -10$ and 10 are constant for the longitudinal rolls, but rate of increase of Ra_T for the transverse rolls for $Ra_S = 10$ is slower than that for $Ra_S = -10$.

In Fig. 3(a), for $Q = 0$, it is also observed that for the negative value of Ra_S, the threshold values of thermal Rayleigh number, Ra_T obtained from linear and nonlinear theories coincide, and hence the region of subcritical instability does not exist. But for the positive value of Ra_S,

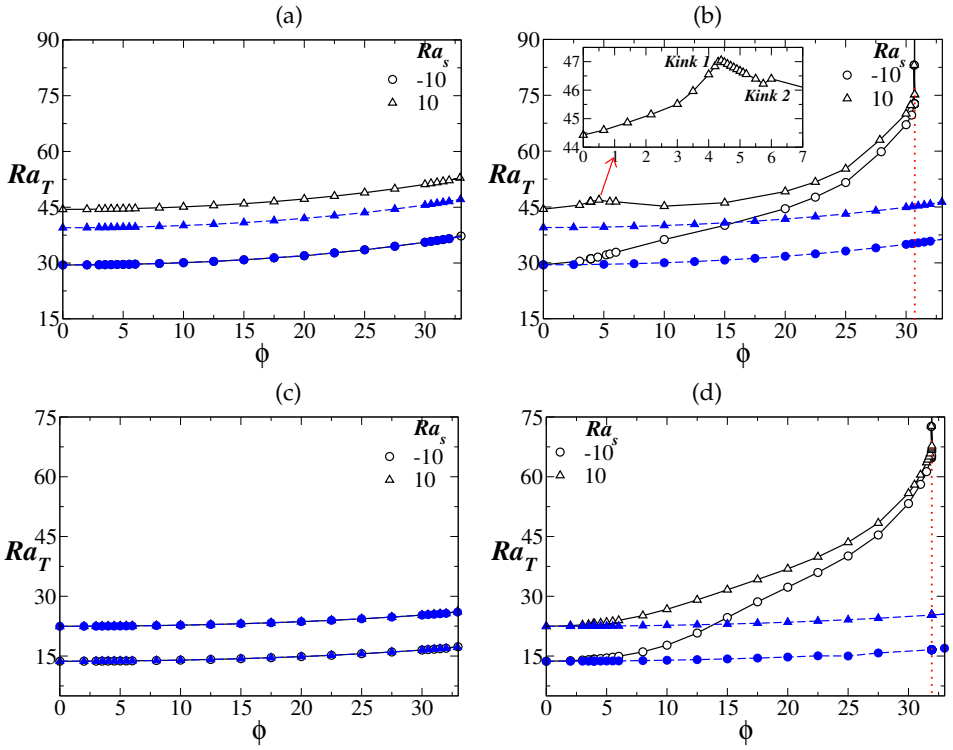

Figure 3. Variations of the threshold thermal Rayleigh number (Ra_T) as a function of angle of inclination of the channel (ϕ) for different values of the solutal Rayleigh number (Ra_S) obtained using the linear instability analysis (open black symbols) and the nonlinear stability analysis (filled blue symbols). The value of the Lewis number (Le) is 10. (a,b) $Q = 0$ and (c,d) $Q = 2$, such that (a,c) are for the longitudinal rolls and (b,d) are for the transverse rolls.

the region of subcritical instability exists and further, an increase in the inclination angle of the porous layer does not alter this region. However, in the case of the transverse rolls (Fig. 3(b)), for the negative value of Ra_S, the region of subcritical instability is negligible for small value of ϕ but it increases as ϕ increases. For the positive value of Ra_S, the area of subcritical instability exists and it widens as the value of ϕ increases. This suggests that the angle of inclination of the channel is important to understand the existence of the subcritical instability region in the system.

Figs. 3(c,d) show the variation of the threshold Rayleigh number Ra_T for both the longitudinal and transverse rolls in the presence of concentration based internal heat source with $Q = 2$. The instability curves in Figs. 3(c,d) for the longitudinal and transverse rolls follow the same pattern as those observed in Figs. 3(a) and (b), respectively. However, the presence of concentration based internal heat source $(Q = 2)$ reduces the threshold value of Ra_T for each value of Ra_S. In this case, the transverse rolls are stationary modes for the entire range of ϕ considered, which is in contrast to the observation made in Fig. 3(b) for $Q = 0$. It can be noted that the stationary transverse rolls are more stable than the stationary longitudinal rolls with and without the presence of the internal heat source.

In Fig. 3(c), it can also be seen that for all values of the solutal Rayleigh number Ra_S (i.e $Ra_S = -10$ and $Ra_S = 10$) the region of subcritical instability does not exist and the linear instability analysis is sufficient to predict the onset of convection for the longitudinal rolls. However, for the transverse rolls (Fig. 3(d)), the region of subcritical instability for small values of ϕ is negligible. But an increment in the inclination angle ϕ increases the region of subcritical instability.

In Figs. 3(b,d), we found that the values of the threshold angle (marked by the red dotted line) below which the transverse rolls due to the double-diffusive convection exist are 30.7° and 31.92°

for $Q = 0$ and $Q = 2$, respectively. In the mono-diffusive case with $Q = 0$, Rees and Bossom [19] and Rees and Barletta [21] have found the threshold inclination angle for the transverse rolls to be $\phi \approx 31.49^\circ$ and $\phi \approx 32.54^\circ$, respectively.

Figs. 4(a,b) and (c,d) depict the variation of the threshold thermal Rayleigh number, Ra_T for the linear instability against the solutal Rayleigh number, Ra_S for different values of angle of inclination, ϕ for $Q = 0$ and $Q = 2$ when $Le = 10$. It can be seen in Fig. 4(a) $(Q = 0)$ that for $Ra_S < 0$, an increase in the value of the inclination angle, ϕ increases the threshold thermal Rayleigh number for the longitudinal rolls up to $Ra_S \approx 5$ and subsequently, for $Ra_S \geq 5$, the threshold value of Ra_T becomes almost constant. This shows that the solutal Rayleigh number has a stabilising effect on the system for $Le = 10$.

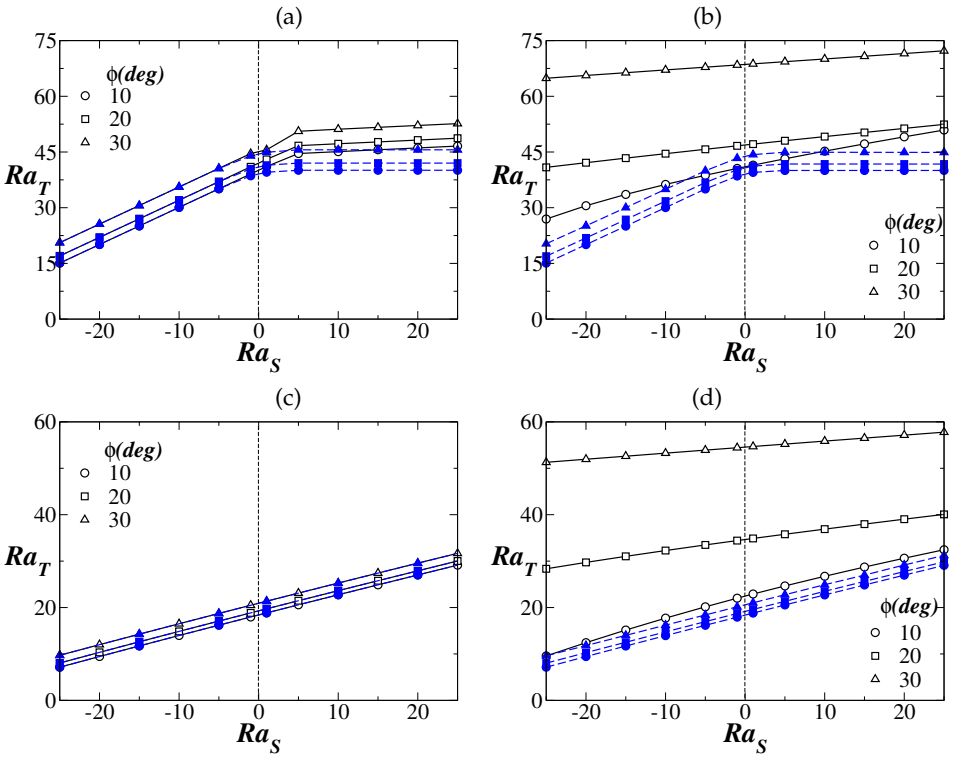

Figure 4. Variations of the threshold thermal Rayleigh number (Ra_T) versus the solutal Rayleigh number (Ra_S) for different values of the angle of inclination of the porous layer obtained using the linear instability analysis (open black symbols) and the nonlinear stability analysis (filled blue symbols). The value of the Lewis number (Le) is 10. (a,b) $Q = 0$ and (c,d) $Q = 2$, such that (a,c) are for the longitudinal rolls and (b,d) are for the transverse rolls.

In the case of the transverse rolls for $Q = 0$ (Fig. 4(b)), increasing the value of Ra_S from $Ra_S = -25$ to $Ra_S = 25$ increases the thermal Rayleigh number and it is higher than the corresponding threshold observed in the case of the longitudinal rolls (Fig. 4(a)). This indicates that the stationary transverse rolls are more preferred to stationary longitudinal rolls. In Figs. 4(c,d) (for $Q = 2$), it can be seen that the threshold values of Ra_T for both the longitudinal and transverse rolls are lower than those observed for $Q = 0$. This can be because increasing the internal heat source increases the global temperature of the system and forces the system into the initiation of convection. It is to be noted that an increment in Ra_S from a negative value to a positive value increases the threshold value of Ra_T when thermal diffusion is much higher than the solutal diffusion. The threshold value of Ra_T in the longitudinal rolls is less as compared to the transverse rolls for all values of ϕ considered. We can, therefore, conclude that transverse rolls are more stable than

longitudinal rolls and that transverse stationary rolls are the preferable mode of instability at the onset of convection.

It is clear from the nonlinear analysis that the stability curves follow a similar trend as the linear instability curves for the longitudinal rolls as shown in Fig. 4(a) in the absence of Q. It is interesting to note that when $Ra_S < 0$, both theories yield the same thresholds for any angle of inclination. However, the linear and nonlinear results differ for $Ra_S > 0$, and increasing Ra_S (for $Ra_S > 0$) enhances the region of subcritical instability. The region of subcritical instability for the longitudinal rolls does not appear for $Q = 2$. For the transverse rolls Fig. 4(b) with $Q = 0$, increasing Ra_S (for $Ra_S < 0$), the nonlinear threshold increases similar to the linear threshold, but the region of subcritical instability decreases as the inclination angle increases. For $Ra_S > 0$, the region of subcritical instability increases with increasing ϕ. A similar kind of observation is seen even in the presence of the concentration based internal heat source Q in Fig. 4(d) for transverse rolls.

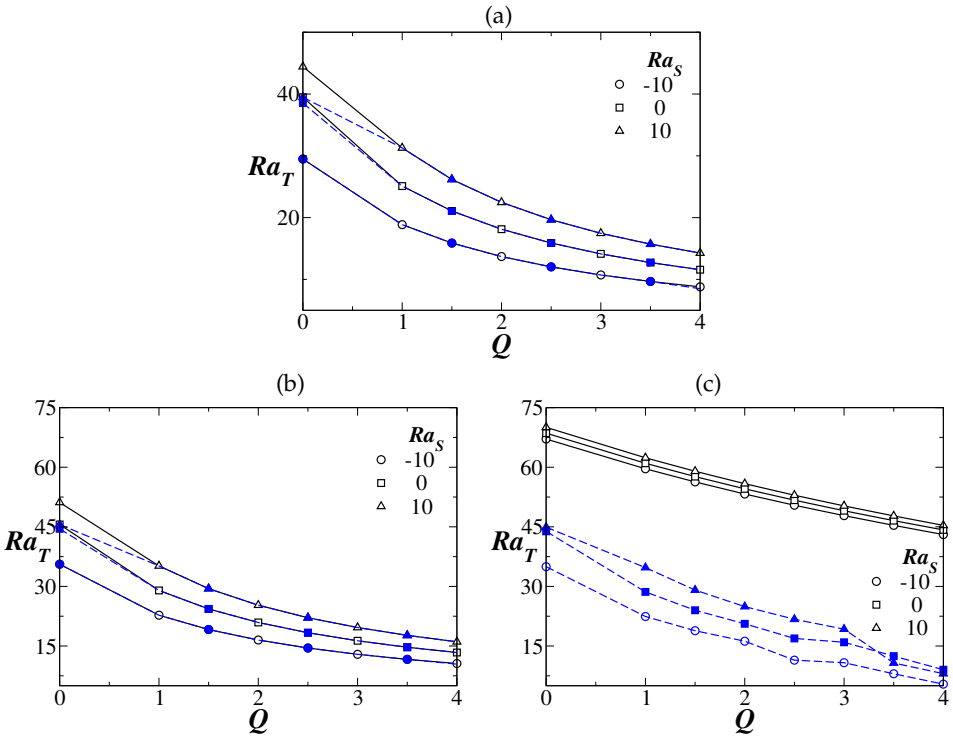

Figure 5. Variations of the threshold thermal Rayleigh number (Ra_T) versus Q different values of the solutal Rayleigh number (Ra_S) obtained using the linear instability analysis (open black symbols) and the nonlinear stability analysis (filled blue symbols). (a) $\phi = 0$ and (b) $\phi = 30^\circ$ (the longitudinal rolls) and (c) $\phi = 30^\circ$ (the transverse rolls). The value of the Lewis number is $Le = 10$. Note that the longitudinal and transverse rolls are the same for $\phi = 0$.

Fig. 5(a) represents the variation of the threshold value of thermal Rayleigh number, Ra_T against the concentration based internal heat source, Q for different values of Ra_S for $\phi = 0$ (horizontal channel) for $Le = 10$. It can be seen in Fig. 5(a) that the instability threshold at the onset for both the longitudinal and transverse rolls coincide. It can also be observed that increasing Ra_S increases the threshold value of Ra_T and increasing Q reduces the threshold value of Ra_T due to the rise in the global temperature of the system. Figs. 5(b,c) represent the longitudinal and transverse rolls for $\phi = 30^\circ$. In Fig. 5(b), we observed that it follows a similar trend as in Fig. 5(a) and the threshold value of Ra_T for $\phi = 30^\circ$ is higher than that for $\phi = 0$ for both the longitudinal rolls and transverse rolls. Inspection of Figs. 5(b,c) also reveals that increasing Ra_S increases the

linear threshold for both the stationary longitudinal and the stationary transverse rolls. Also, the stationary transverse rolls are more stable than the stationary longitudinal rolls, but for the high value of Ra_S, the stationary transverse rolls are preferable over the stationary longitudinal rolls.

For $\phi = 0^\circ$ (Fig. 5(a)) and for the longitudinal rolls at $\phi = 30^\circ$ (Fig. 5(b)), the linear and the nonlinear theories give the same threshold Ra_T values, except for $Ra_S = -10$ and $Q < 1$ indicating that the subcritical instability exists only for $Ra_S = -10$ and $Q < 1$. For $\phi = 30^\circ$, in the case of transverse rolls (Fig. 5(c)) the region of subcritical instability exists for all values of Ra_S considered.

4. Concluding remarks

In this study, using linear instability and nonlinear stability (energy functional) analyses, we investigate the double-diffusive instability in an inclined porous layer with and without an internal heat source based on concentration. The thermal Rayleigh number (Ra_T), solutal Rayleigh number (Ra_S), angle of inclination of the porous surface (ϕ), Lewis number (Le), and concentration-based internal heat source (Q) are the dimensional parameters that govern the dynamics considered in the present work. The region of subcritical instability for longitudinal and transverse rolls has been analysed for different dimensionless parameters by comparing the threshold values of Ra_T obtained from linear and nonlinear theories. We found linear instability and the region of subcritical instability which arise due to the differential diffusivity of the temperature and concentration, and the presence of the internal heat source based on concentration. For a high value of Le, the temperature of the system at the interior tends to become uniform, thereby increases the gradient of temperature near the walls. Also increasing the strength of the internal heat source based on concentration increases the temperature of the system. These phenomena are found to destabilise the system.

The angle of inclination (ϕ) is a crucial parameter in the present study. It is observed that both stationary and oscillatory modes occur in an inclined double-diffusive porous layer as considered in this study which contrasts clearly with the mono-diffusive system, where the only preferred mode is the stationary one [19]. In particular, for the set of parameters considered, we found that for the transverse roll with $Q = 0$, the stationary transverse rolls exist between $\phi = 0^\circ$ and $\phi \approx 4^\circ$, but at around $\phi \approx 4^\circ$, the convection switches from the stationary transverse rolls to the travelling transverse rolls. Again for $\phi > 5.7^\circ$ (approximately) the convective instability is in the form of the stationary transverse rolls. We also found that the values of the threshold inclination angle below which the transverse rolls due to the double-diffusive convection exist are 30.7° and 31.92° for $Q = 0$ and $Q = 2$, respectively. The angle of inclination (ϕ) of the channel is found to increase the onset threshold value and thereby stabilising the system in both the linear and nonlinear stability analyses. It is observed that the regions of subcritical instability increases as the inclination of the porous layer, ϕ increases due to the reduction of the effective gravity in the wall-normal direction.

For all inclination angles considered, the threshold values of the longitudinal rolls obtained from both the linear and nonlinear theories coincide for $Ra_S < 0$ and $Le = 10$, and thus the region of subcritical instability does not exist for $Ra_S < 0$. This region disappears when the internal heat source Q is present. This is in contrast to the observations made for the transverse rolls, where, even in the absence of (Q), the region of subcritical instability exists. For low values of Le and Q, the region of subcritical instability is observed even for the longitudinal rolls .

Acknowledgment

G. K. would like to acknowledge the research fellowship provided by the Council of Scientific and Industrial Research (CSIR), Government of India through the grant number: 09/1001(0022)/2016-EMR-I. The authors acknowledged the constructive suggestiongs of the anonymous reviewers.

References

1. Bendrich G, Shemilt LW. 1997 Mass transfer in horizontal flow channels with thermal gradients. *Can. J. Chem. Eng.* **75**, 1067–1074.
2. Radko T. 2013 *Double-diffusive convection*. Cambridge University Press.
3. Mishra M, Trevelyan PMJ, Almarcha C, Wit DA. 2010 Influence of double diffusive effects on miscible viscous fingering. *Phys. Rev. Lett.* **105**, 204501.
4. Govindarajan R, Sahu KC. 2014 Instabilities in viscosity-stratified flow. *Ann. Rev. Fluid Mech.* **46**, 331–353.
5. Sahu KC. 2014 A review on double-diffusive instability in viscosity stratified flows. *Proc. Indian Natn. Sci. Acad.* **80**, 513–514.
6. Sahu KC, Govindarajan R. 2011 Linear stability of double-diffusive two-fluid channel flow. *J. Fluid Mech.* **687**, 529–539.
7. Turner J. 1974 Double-diffusive phenomena. *Ann. Rev. Fluid Mech.* **6**, 37–54.
8. Trevisan OV, Bejan A. 1990 Combined heat and mass transfer by natural convection in a porous medium. *Advances in Heat Transfer* **20**, 315–352.
9. Parthiban C, Patil PR. 1995 Effect of non-uniform boundary temperatures on thermal instability in a porous medium will] internal heat source. *Int. Commun. Heat Mass* **22**, 683–692.
10. Parthiban C, Patil PR. 1997 Thermal instability in an anisotropic porous medium with internal heat source and inclined temperature gradient. *Int. Commun. Heat Mass Transfer* **24**, 1049–1058.
11. Rionero S, Straughan B. 1990 Convection in a porous medium with internal heat source and variable gravity effects. *Int. J. Eng. Sci.* **28**, 497–503.
12. Alex SM, Patil PR. 2002 Effect of a variable gravity field on convection in an anisotropic porous medium with internal heat source and inclined temperature gradient. *J. Heat Transfer* **124**, 144–150.
13. Hill AA. 2005 Double–diffusive convection in a porous medium with a concentration based internal heat source. *Proc. Royal Soc. A* **461**, 561–574.
14. Capone F, Gentile M, Hill AA. 2011 Double-diffusive penetrative convection simulated via internal heating in an anisotropic porous layer with throughflow. *Int. J. Heat Mass Transf.* **54**, 1622–1626.
15. Gautam K, Narayana PAL. 2019 On the stability of carbon sequestration in an anisotropic horizontal porous layer with a first-order chemical reaction. *Proc. R. Soc. Lond. A* **475**, 20180365.
16. Bories SA, Combarnous MA. 1973 Natural convection in a sloping porous layer. *J. Fluid Mech.* **57**, 63–79.
17. Caltagirone JP, Bories S. 1985 Solutions and stability criteria of natural convective flow in an inclined porous layer. *J. Fluid Mech.* **155**, 267–287.
18. Weber JE. 1974 Thermal convection in a tilted porous layer. *Preprint series. Mechanics and Applied Mathematics http://urn. nb. no/URN: NBN: no-23418*.
19. Rees DAS, Bassom AP. 2000 The onset of Darcy-Bénard convection in an inclined layer heated from below. *Acta Mechanica* **144**, 103–118.
20. Barletta A, Storesletten L. 2011 Thermoconvective instabilities in an inclined porous channel heated from below. *Int. J. Heat Mass Transf.* **54**, 2724–2733.
21. Rees DAS, Barletta A. 2011 Linear instability of the isoflux Darcy–Bénard problem in an inclined porous layer. *Transport Porous Med.* **87**, 665–678.
22. Vasseur P, Satish MG, Robillard L. 1987 Natural convection in a thin, inclined, porous layer exposed to a constant heat flux. *Int. J. Heat Mass Transf.* **30**, 537–549.
23. Sen M, Vasseur P, Robillard L. 1987 Multiple steady states for unicellular natural convection in an inclined porous layer. *Int. J. Heat Mass Transf.* **30**, 2097–2113.
24. Barletta A, Rees DAS. 2012 Linear instability of the Darcy–Hadley flow in an inclined porous layer. *Phys. Fluids* **24**, 074104.
25. Nield DA, Barletta A, Celli M. 2011 The effect of viscous dissipation on the onset of convection in an inclined porous layer. *J. Fluid Mech.* **679**, 544–558.
26. Ingham DB, Pop I. 1998 *Transport phenomena in porous media*. Elsevier.
27. Nield DA, Bejan A. 2013 *Convection in porous media*. Springer 4 edition.
28. Vafai K. 2015 *Handbook of porous media*. CRC Press.
29. Barletta A, Celli M, Nield DA. 2014 Unstable buoyant flow in an inclined porous layer with an internal heat source. *Int. J. Therm. Sci.* **79**, 176–182.
30. Matta A, Hill AA. 2018 Double-diffusive convection in an inclined porous layer with a concentration-based internal heat source. *Continuum Mech. Thermodyn.* **30**, 165–173.

31. Joseph DD. 2013 *Stability of fluid motions I* vol. 27. Springer Science & Business Media.
32. Straughan B. 2008 *Stability and wave motion in porous media* vol. 165. Springer Science & Business Media.
33. Straughan B. 2013 *The energy method, stability, and nonlinear convection* vol. 91. Springer Science & Business Media.
34. Wen B, Chini GP. 2018 Inclined porous medium convection at large Rayleigh number. *J. Fluid Mech.* **837**, 670–702.
35. Falsaperla P, Mulone G. 2018 Thermal convection in an inclined porous layer with Brinkman law. *Ricerche di Matematica.* **67**, 983-999.
36. Falsaperla P, Giacobbe A, Mulone G, 2019 Inclined convection in a porous Brinkman layer: linear instability and nonlinear stability. *Proceedings of the Royal Society A.* **475**, 20180614.
37. Dongarra JJ, Straughan B, Walker DW. 1996 Chebyshev tau-QZ algorithm methods for calculating spectra of hydrodynamic stability problems. *Appl. Numer. Math.* **22**, 399–434.
38. Straughan B, Walker DW. 1996 Two very accurate and efficient methods for computing eigenvalues and eigenfunctions in porous convection problems. *J. Comput. Phys.* **127**, 128–141.
39. Nield D, Manole D, Lage J. 1993 Convection induced by inclined thermal and solutal gradients in a shallow horizontal layer of a porous medium. *J. Fluid Mech.* **257**, 559–574.
40. Schmid PJ, Henningson DS. 2001 *Stability and transition in shear flows*. New York: Springer-Verlag New York, Inc.
41. Gautam K, Narayana PAL, Hill AA. 2019 Thermo-convective carbon sequestration in horizontal porous layers. *IMA J. Appl. Math.* **84**, 650–668.